Semiconductors, 2024, Vol. 58, No. 8

Electrical Properties of Highly Nitrogen-Doped Synthetic Single Crystal Diamonds Grown at High Pressure and Temperature

© S.G. Buga[1,2], I.N. Kupriyanov[3], Yu.M. Borzdov[3], M.S. Kuznetsov[1], N.V. Luparev[1], S.A. Nosukhin [1], B.A. Kulnitskiy[1,2], D.D. Prikhodko[1,2], Yu.N. Palyanov[3]

[1] Technological Institute for Superhard and Novel Carbon Materials,
108840 Moscow, Russia
[2] Moscow Institute of Physics and Technology,
141701 Dolgoprudny, Moscow region, Russia
[3] Sobolev Institute of Geology and Mineralogy, Siberian Branch Russian Academy of Sciences,
630090 Novosibirsk, Russia

E-mail: buga@tisnum.ru

Received September 8, 2024
Revised October 6, 2024
Accepted October 29, 2024

Using the temperature gradient method at high pressure and temperature (TG-HPHT), we have grown 3 diamond single crystals from growth media Co−Fe−C−N and Ni−Fe−C−N with a concentration of singly substitutional nitrogen atoms (C centers) in the range $(0.7-1.35)\cdot 10^{20}\,\mathrm{cm}^{-3}$. Samples were made from 2 of them for the study of electrical properties by the Hall effect method in van der Pauw geometry. The dependences of the resistivity and the Hall coefficient on temperature are investigated, by which the temperature dependences of the concentration of free electrons and their Hall mobility are calculated. For a sample with a concentration of C centers $\sim 10^{20}\,\mathrm{cm}^{-3}$, the temperature dependence of electrical conductivity was investigated. At $T > 650\,\mathrm{K}$, linear sections of $\ln(\sigma)$ dependences on the inverse temperature $1/T$ are observed, on the basis of which the activation energies of conductivity 1.5−1.64 eV are determined, higher than those of previously studied samples with a lower nitrogen concentration grown by the same method. In samples with C-center concentrations of $0.7\cdot 10^{20}$ and $1.35\cdot 10^{20}\,\mathrm{cm}^{-3}$, the dependences of $\ln(n)$ on $1/T$ are linear throughout the studied temperature range. Based on them, the values of donor ionization energy $E_d = 1.32$ eV; 1.53 eV, and compensation ratios equal to $k = 25$ and 45% are calculated, which are significantly higher than the values for diamonds with a lower nitrogen concentration studied before. It is assumed that the acceptors are iron atoms, complexes of iron and nitrogen atoms in the substitutional position, complexes of iron atoms with vacancies, as predicted theoretically, as well as similar impurity centers based on nickel and cobalt atoms.

Keywords: *n*-type semiconductor diamond, nitrogen doping, electrical resistance, Hall mobility of free electrons, ionization energy of donors, activation energy of conductivity.

DOI: 10.61011/SC.2024.08.59889.7054

1. Introduction

Diamond doped with nitrogen in the substitutional position N_s (N_s is the nitrogen concentration) is a wide-band *n*-type semiconductor [1–3], and the applications of such synthetic diamond single crystals, which are known as type Ib diamonds [1,4], in electronics and optoelectronics are being studied actively at present. A thin (10 nm) nitrogen-doped layer was used to produce a $p-n$ junction in a *p*-type composite Schottky diode operating at temperatures up to 1000°C in vacuum [5]. Nitrogen-doped diamond layers were used in a Schottky $p-n$ diode [6], an inversion *p*-channel MOS transistor [7], single-photon *pin* diodes [8], and high-temperature light-emitting *pin* diodes [9]. New signal processing techniques provide an opportunity to use type Ib diamonds in modern high-dose radiation therapy, where conventional dosimeters have certain limitations [10].

The dependences of concentration of free electrons and their mobility were examined in our study [3] by the Hall effect method within the 550−1143 K temperature range at a nitrogen dopant concentration of $(10^{18}-6.5)\cdot 10^{19}\,\mathrm{cm}^{-3}$. It was found that, in accordance with the trend observed in other semiconductors, donor ionization energy E_d decreases to a minimum of 1.33 ± 0.01 eV with an increase in their concentration N_d. Specifically, a dependence of this kind for diamonds doped with phosphorus was analyzed in [11]. In the case of diamond doping with boron, concentration transitions to the degenerate semiconductor state, a semiconductor−semimetal transition, and a transition to the superconducting state at low temperatures are observed at concentrations $> 3\cdot 10^{20}\,\mathrm{cm}^{-3}$ [12,13]. Such heavily boron-doped diamonds provide an opportunity to form fine ohmic contacts to *p*-type diamond. Nitrogen-doped type Ib diamonds are also of interest in the context of advancement of diamond electronics. The ionization energy of donors in them should be significantly lower than 1.7 eV, and they may have sufficiently high concentration and mobility of free electrons. The trend of E_d reduction and growth of the concentration of free electrons observed in [3] should naturally continue with a further increase in N_s. However, E_d for the sample with the highest concentration N_s turned out to be noticeably higher $(1.41\pm 0.03\,\mathrm{eV})$. The reason for this

deviation is unclear, and further studies are needed to clarify the dependence of the energy of ionization of donor nitrogen atoms on their concentration at $N_s > 6.5 \cdot 10^{19}\,\mathrm{cm}^{-3}$. The study of electrical properties of heavily nitrogen-doped type Ib diamonds is also of interest in the context of their superconductivity, which was predicted theoretically (in much the same way as for boron-doped diamonds [14–16]) at a dopant concentration greater than $\sim 10^{21}\,\mathrm{cm}^3$. The first signs of local superconductivity of nitrogen-doped diamonds have already been observed in [17–19] at concentrations $N_s < 6 \cdot 10^{19}\,\mathrm{cm}^{-3}$. However, it is rather difficult to grow sufficiently large single crystals of type Ib diamond with high concentration $N_s > 6.5 \cdot 10^{19}\,\mathrm{cm}^{-3}$ and a low concentration of defects in the form of paired nitrogen atoms (A-centers). In general, the study of electrical properties of heavily nitrogen-doped type Ib diamond single crystals is relevant both to determining the possibilities of practical application of such crystals and to improving their growth methods.

It was established in [3] that the lowest compensation ratio $k = N_a/N_d < 1\%$, where N_a is the acceptor concentration, corresponds to diamonds with a low level of nitrogen doping $\sim 10^{18}\,\mathrm{cm}^{-3}$ produced by the homoepitaxial growth method on a single-crystal diamond substrate from the vapor phase (CVD method). Single crystals of diamond with nitrogen concentrations within the $(0.95-6.5) \cdot 10^{19}\,\mathrm{cm}^{-3}$ range grown by the temperature gradient method at high pressure and temperature (TG-HPHT) [20] have a fairly significant fraction of acceptors ($\sim 10-20\%$), and one of the samples even had a significantly higher value of $k \sim 37\%$. It should be noted that the calculations in [3] were performed under the approximation that Hall scattering factor γ, which is equal to the ratio of the drift mobility of free carriers to the Hall mobility, assumes a value of 1. Theoretical estimates of γ in [21] suggest a more correct value of $\gamma = 1.5 \pm 0.3$. The same value follows from a comparison of the mobilities of free electrons in phosphorus-doped diamonds [22] and holes in boron-doped diamonds [23] measured by the time-of-flight method and the Hall effect method. The use of this γ value leads to a slight reduction in k for the experimental data [3] to $(6-12)\%$ in all diamond samples grown by the TG-HPHT method (except for the sample with the highest $k = 30 \pm 5\%$). The nature of acceptor states is not entirely clear in this case, since the main acceptor in diamonds is boron, but the concentration of boron in the studied diamonds was $< 10^{16}\,\mathrm{cm}^{-3}$ (i.e., no less than 2 orders of magnitude lower than the concentration of nitrogen donors). When the HPHT method is used, diamond single crystals are produced from a solution of carbon in melts of transition metals (primarily iron with cobalt, nickel, and manganese additives). The concentration of metallic impurities in high-quality single crystals may be quite low. For example, it was $(0.5-1.5) \cdot 10^{18}\,\mathrm{cm}^{-3}$ in the samples examined in [17–19], but the role of impurities in the process of carrier transport remains understudied.

The density functional method was used in a recent theoretical study [24] to simulate possible energy levels of iron atoms, complexes of iron and nitrogen atoms in the substitutional position ($\mathrm{Fe}_s-\mathrm{N}_s$), and complexes of iron atoms with vacancies in a diamond supercell of 1000 atoms. It was demonstrated that such complexes may have acceptor properties. Metal nitrides (e.g., $\mathrm{Fe_3N}$) are used both as an additive to the solvent catalyst and as a growth medium to increase the nitrogen concentration in HPHT-grown diamonds [25,26]. This provides an opportunity to raise the concentration of nitrogen atoms in the substitutional position to $N_s \sim 1.4 \cdot 10^{20}\,\mathrm{cm}^{-3}$. It is of interest to determine how the increase in concentration of nitrogen donors provided by this growth method affects the electrical properties of diamonds (specifically, the concentration of acceptors). Thus, the aim of the present study was to examine the electrical properties of HPHT-grown single-crystal diamond samples with nitrogen concentration N_s within the $(0.7-1.4) \cdot 10^{20}\,\mathrm{cm}^{-3}$ range and to compare the obtained results with the data reported earlier in [3].

2. Experimental samples and measurement procedure

Three diamond single crystals were grown using the temperature gradient method at high P, T (TG-HPHT). Crystal #ND-2 was grown in a high-pressure „toroid“ setup in the Fe–Co–C–N system [19]. Crystals #185 and #443 were produced using a BARS press-free high-pressure „split sphere“ apparatus [20] in the Ni–Fe–C–N (#185) and Co–Fe–C–N (#443) systems [26]. Pure chemical compounds were used to avoid accidental contamination of grown diamonds with other impurities. Two square-shaped samples were formed by laser cutting and mechanical polishing from crystals #ND-2 and #185 for subsequent studies of electrical properties by Hall effect measurements in the van der Pauw geometry (Figures 1, *a* and *b*).

The samples were cleaned from surface contamination by etching in a boiling mixture of hydrochloric and nitric acids (3 : 1 by volume) for 2 h with subsequent rinsing in deionized water and annealing in atmosphere at $T = 680^\circ\mathrm{C}$ for 20 min. Following this, layers of Ti with a thickness of 5 nm and Pt with a thickness of 200 nm were deposited by magnetron sputtering through contact masks. Annealing was performed in vacuum ($10^{-5}-10^{-6}$ Torr) at $T = 650^\circ\mathrm{C}$ for 20 min after the deposition of Ti and Pt layers to form titanium carbide. This ensured linearity of the current–voltage characteristics within a wide range of temperatures up to ~ 1000 K. The Pt layer prevents oxidation of titanium in air and maintains good adhesion in the process of subsequent heating during measurements. Such contacts of a finite area provide a reduction in contact resistance and are suitable for investigating the electrical characteristics of nitrogen-doped diamond single crystals by the van der Pauw method [27]. Electrical contacts to the third crystal (#443) were fabricated in a similar manner; the difference was that two contacts were formed on opposite planar growth faces (111) of the crystal (see

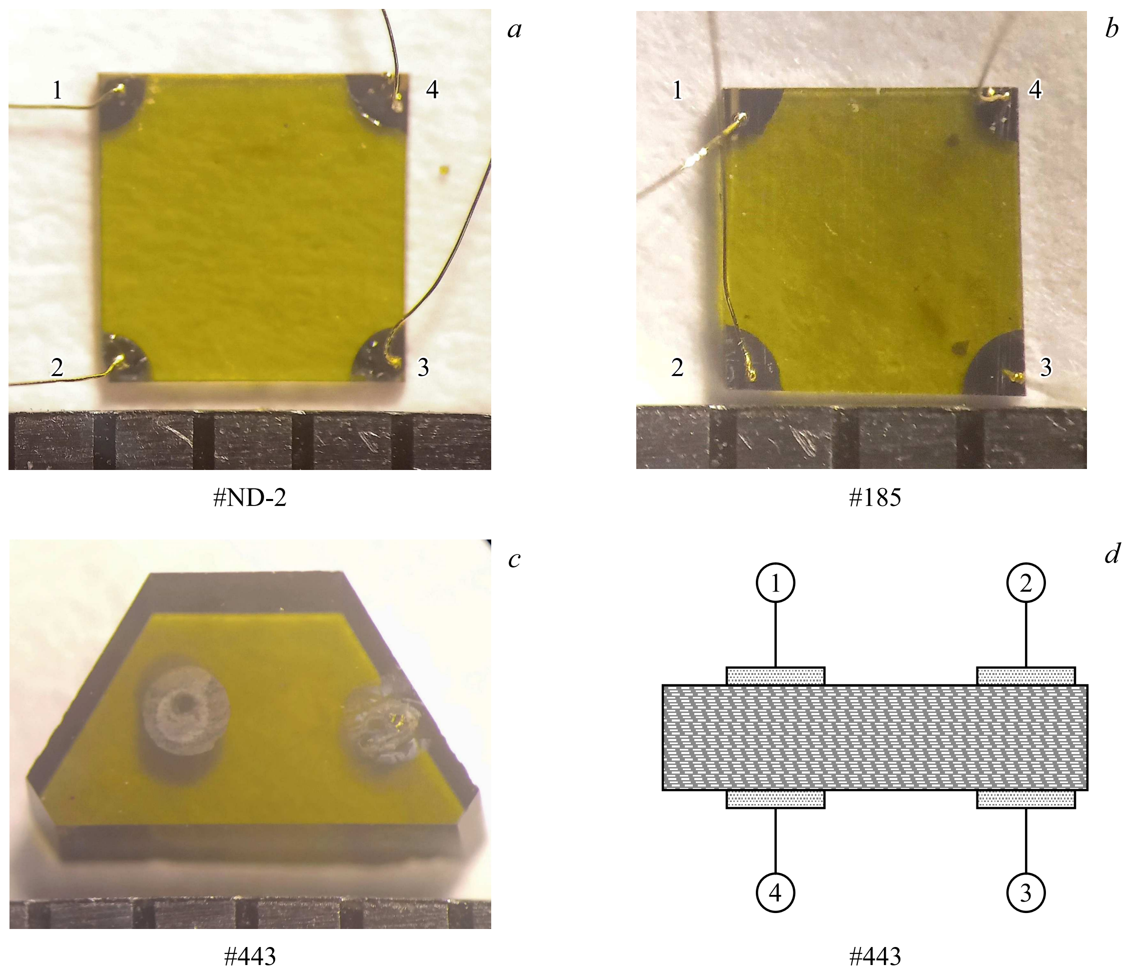

Figure 1. *a, b* — Photographic images of experimental samples #ND-2 and #185 cut from nitrogen-doped diamond single crystals with corner contacts and welded gold microwires for resistivity measurements by the van der Pauw method. *c* — Photographic image of sample #443; *d* — cross-sectional diagram of sample #443 with 4-contact pads on opposite sides for 4-point resistance measurements. A scale with 1 mm divisions is shown at the bottom in panels (*a*–*c*).

Parameters of the studied samples *

Sample number	Size, mm^3	Crystallographic orientation	N_c (C-centers), 10^{20} cm^{-3}	N_2 (A-centers), 10^{20} cm^{-3}	k, %	$E_a(\sigma)$, eV (±0.01 eV)	E_d, eV (±0.01 eV)
#CVD [3]	$2.5\times2.5\times0.25$	(100)	0.0085 ± 0.1	–	0.7 ± 0.2	1.55	1.63
#2 [3]	$4.0\times4.0\times0.43$	(100)	0.24 ± 0.02	<0.01	14 ± 3	1.35	1.38
#5 [3]	$4.0\times4.0\times0.07$	(100)	0.5 ± 0.2	<0.002	30 ± 4	1.32	1.33
#ND-2	$3.0\times3.0\times0.20$	(111)	0.7 ± 0.03	0.07 ± 0.02	25 ± 5	1.50	1.32
#185	$2.5\times2.5\times0.25$	(111)	1.35 ± 0.04	0.09 ± 0.02	45 ± 5	1.63	1.53
#443	$4.0\times2.5\times0.7$	(111)	1.02 ± 0.04	0.07 ± 0.02	$*$	1.64	$*$

Note. * The sizes of experimental samples and their crystallographic orientation, concentrations N_c of donor C-centers, concentrations N_2 of neutral A-centers, compensation ratio k calculated using Eq. (2), activation energy of electrical conductivity $E_a(\sigma)$, and donor activation energy E_d. The data for samples #CVD, #2, and #5 from [3] are given for comparison. Symbols $*$ indicate lack of data.

the photo and diagram in Figures 1, *c* and *d*). Only the dependence of electrical resistance on temperature was examined in this case in 2-point and 4-point arrangements. Electrical leads in the form of $\varnothing 40\,\mu$m gold wires were welded to the fabricated contact pads by thermocompression bonding.

Prior to electrical measurements, IR absorption spectra were measured to estimate the concentration of donor nitrogen atoms (C-centers) and other optically active nitrogen centers, such as A-centers and N^+-centers [28–30]. The obtained IR spectra are shown in Figure 2, *a*. Figure 2, *b* presents an example mathematical decomposition of the IR

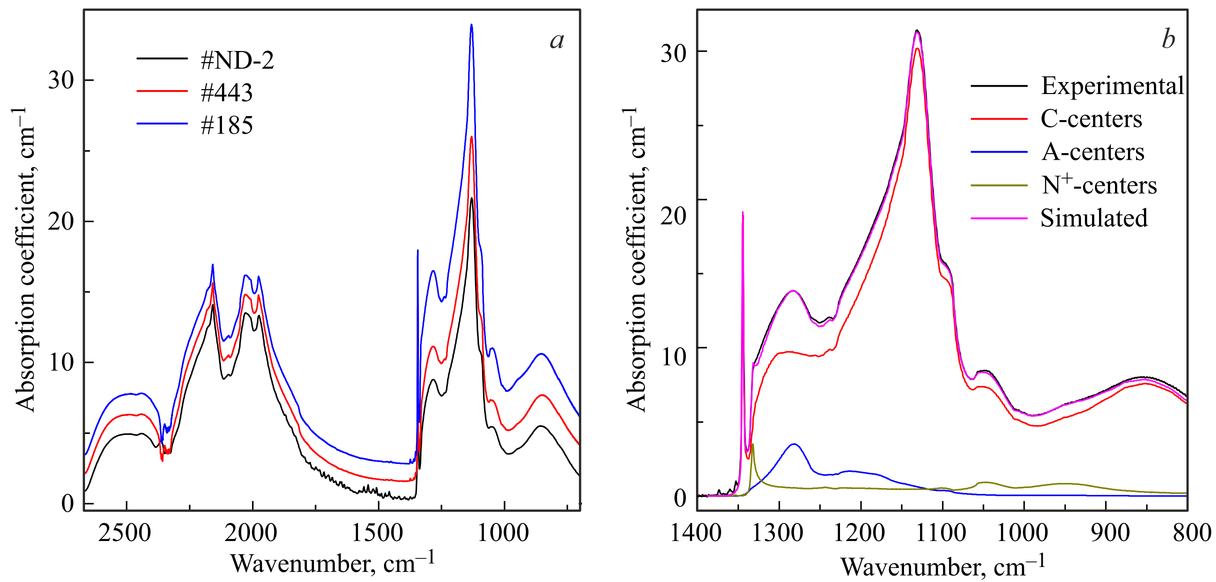

Figure 2. *a* — IR absorption spectra: black curve — sample #ND-2; red curve — #443; blue curve — #185. The spectra are shifted along the vertical axis for clarity. (*b*) — Example decomposition of the absorption spectrum of sample #185 in the single-phonon region into components corresponding to the spectra of C-, A-, and N$^+$-centers. (A color version of the figure is provided in the online version of the paper).

spectrum of sample #185 in the nitrogen absorption region into components corresponding to C-, A-, and N$^+$-centers. The absolute values of concentrations of nitrogen centers in the samples are listed in the table.

The local concentration of iron and nickel metal impurities from the growth medium was also measured in sample #185 with the highest nitrogen concentration using an energy-dispersive spectrometer (EDS) coupled with a JEM-2010 transmission electron microscope. The focal spot diameter of the electron beam was ~ 50 nm, and spectra were recorded at 15 randomly selected points on a particle of the given sample of a micrometer size. The average concentration at ten examined points was ~ 100 ppm for Fe and 200 ppm for Ni, although the corresponding values at the other five points were significantly higher (~ 5000 ppm for Fe and 2000 ppm for Ni). Presumably, metals are in a (partially) dissolved form at most points, and nanoclusters of the Fe–Ni alloy may also be present at certain points.

Just as in our earlier study [3], electrical measurements were performed using a LakeShore™ Cryotronics 7707A HMS Hall effect setup. The samples were heated in an argon atmosphere in a sealed Linkam-1000TS heater, which provided a maximum temperature of 1000°C. A sufficient measurement accuracy was achieved at temperatures $> 250-300$°C when the measured resistance of the samples dropped below 100 GΩ.

Figures 3, 4 present example $I-V$ characteristics of the studied samples measured at different temperatures with 2-point and 4-point connection through different contact pads (the pad numbers are indicated in Figure 1). All these $I-V$ characteristics are linear, which is a necessary condition for examining the temperature dependence of electrical resistance. The slopes of the $I-V$ characteristics corresponding to the values of electrical resistance R_{ijkl} (i, j and k, l are the numbers of current and potential contacts, respectively) determined with connection to pairs of contacts on different sides of square samples #ND-2 and #185 were fairly close. The differences in slopes are attributable to the variation of contact area and, possibly, to a certain spatial non-uniformity in the concentration of donor nitrogen dopant and acceptor centers.

The current–voltage characteristics measured for sample #443 in 2-point and 4-point connection arrangements also remain linear within the entire studied temperature range. Example $I-V$ characteristics measured at $T = 300$ and 630°C are shown in Figure 4. It should be noted that the resistance values determined in opposite 4-point connection arrangements (R_{4213} and R_{1342}) match, indicating high measurement accuracy. However, only the value of sample resistance R was measured this way; it is difficult to calculate with reasonable accuracy the value of resistivity ρ and conductivity σ in such a configuration of contact pads.

3. Experimental results and their analysis

Figure 5 presents the results of measurements of resistivity ρ and Hall coefficient modulus R_{H} as a function of inverse temperature (Figures 5, *a, b*) and the obtained calculated temperature dependences of concentration of free electrons n and Hall mobility μ_{H} (Figures 5, *c, d*). The Hall coefficient is negative, which is indicative of electronic conductivity.

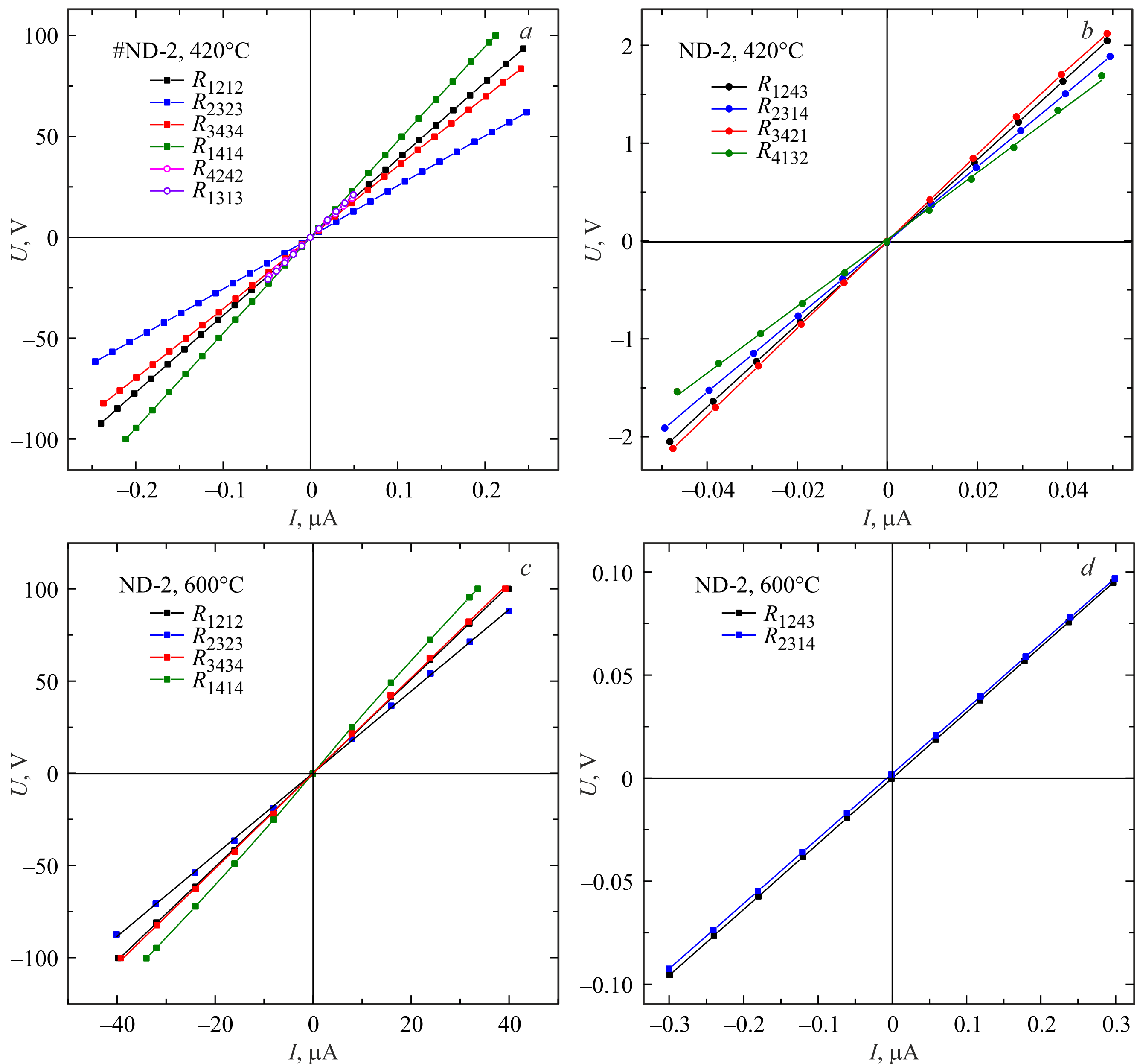

Figure 3. Current–voltage characteristics of sample #ND-2 measured at temperatures of 420 and 600°C in 2-point (a, c) and 4-point (b, d) geometries R_{ijkl}, where$i$, j are the numbers of current contacts and k, l are the numbers of potential contacts (see Figure 1, a).

The value of n was calculated using known relation $n = \gamma/(e|R_\mathrm{H}|)$ for the Hall effect, where γ is the Hall scattering factor and e is the electron charge. As was noted in the Introduction, $\gamma = 1.5 \pm 0.3$ based on the theoretical model [15] and experimental data for phosphorus-doped diamonds [22,23]. The Hall mobility was calculated as $\mu_\mathrm{H} = |R_\mathrm{H}|/\rho$. The data for samples #CVD, #2, and #5 with lower concentrations of nitrogen C-centers from our earlier study [3] are also shown for comparison. It is evident that the value of ρ and the Hall coefficient modulus in samples #ND-2 and #185 with a higher concentration of C-centers remain significantly higher than the corresponding quantities in sample #2 within the entire studied temperature range. Concentration n of free electrons in samples #ND-2 and #185 is $2-3$ times and more than an order of magnitude lower than in sample #2, respectively (Figure 5, c), although the concentration of donor nitrogen atoms in samples #ND-2 and #185 is $\sim 3-5.5$ times higher than the one in sample #2. In addition, the slope of curve $n(1/T)$ in semi-logarithmic coordinates for sample #ND-2 is almost the same as the one for sample #2, while sample #185 exhibits a somewhat greater slope.

It can be seen from Figure 5, d that the significant enhancement of resistivity of samples #ND-2 and #185 compared to #2 is also attributable to significantly lower electron mobility μ_H values, although the value of μ_H for

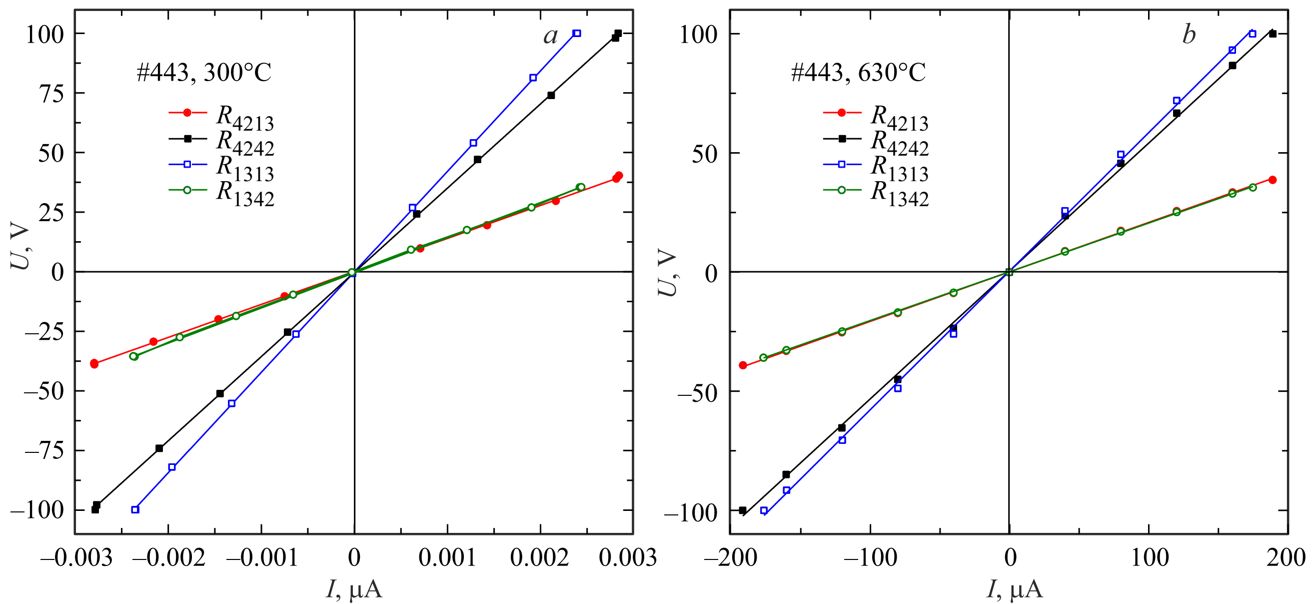

Figure 4. Current–voltage characteristics of sample #433 measured at different temperatures in 2-point (*a*) and 4-point (*b*) geometries R_{ijkl}, where i, j are the numbers of current contacts and k, l are the numbers of potential contacts (see the diagram in Figure 1, *d*).

sample #185 at $T = 600-620$ K is close to the data for sample #2.

Following [3] and earlier studies for phosphorus-doped n-type diamond [31–33], we used a theoretical model of concentration n of free electrons in a partially compensated n-type semiconductor to determine donor ionization energy E_d and compensation ratio $k = N_a/N_d$.

The expression for electron concentration n in a partially compensated n-type semiconductor with Boltzmann statistics and a parabolic conduction band edge is as follows [34]:

$$\frac{g_d n(N_a + n)}{N_c(N_d - N_a - n)} = \exp\left(-\frac{E_d}{k_B T}\right), \quad (1)$$

where $N_c = 2\left(\frac{2\pi m_d^* k_B T}{h^2}\right)^{3/2}$ is the effective density of states in the conduction band, $g_d = 2$ is the donor degeneracy factor, E_d is the donor activation energy, k_B is the Boltzmann constant, and h is the Planck constant. $m_d^* = 6^{2/3} m_\parallel^{1/3} m_\perp^{2/3} = 1.639 m_0$ is the effective mass for the equivalent density of states; according to [35], $m_\parallel = 1.56 m_0$ and $m_\perp = 0.28 m_0$.

Since our experimental data indicate that $n \ll N_d$ and we assume that acceptor concentration N_a is $\geq 1\%$ of N_d, then $n \ll N_a$. The left-hand side of expression (1) may then be simplified, and the resulting shortened expression (2) may be used to calculate E_d and compensation ratio k based on the experimentally obtained $n(T)$ dependencies (as was done in [3,11]):

$$n(T) = \frac{N_c}{g_d}\left(\frac{1}{k} - 1\right)\exp\left(-\frac{E_d}{k_B T}\right). \quad (2)$$

Using Eq. (2), we found the values of E_d and k via two-parameter least-squares fitting to the experimental $n(T)$ data (see Figure 5, *e*, where this was done for sample #185). The results of calculation of E_d and k for samples #ND-2 and #185 are also presented in the table.

Figure 5, *f* shows the dependence of conductivity σ of sample #185 on inverse temperature in semi-logarithmic coordinates that allows one to determine activation energy E_σ of conductivity within the temperature ranges of 570–650 and 800–1020 K. In the high-temperature region, $E_\sigma = 1.63$ eV, which is quite close to the value of 1.7 eV reported by Farrer [1] in his study of the temperature dependence of conductivity of diamond samples cut from a natural type Ib single crystal with a concentration of nitrogen atoms in the substitutional position of $\sim 10^{19}$ cm^{-3} (this concentration was determined by the electron paramagnetic resonance (EPR) method). In addition, a fairly linear section of the dependence of $\lg(\sigma)$ on $1/T$ with activation energy $E_\sigma = 0.73$ eV is observed at temperatures $T < 650$ K in sample #185 (Figure 5, *f*). However, no such section is found in the dependence of $\ln(n)$ on $1/T$ (see Figure 5, *c*). At the same time, it follows from Figure 5, *d* that the electron mobility in this sample at $T < 700$ K is several times higher than at $T > 700$ K. This translates into a strong difference in the shape of dependences of $\ln(\rho)$ and $\ln(n)$ on $1/T$ in Figures 5, *a* and *c* for sample #185. Since the dependence of $\ln(n)$ on $1/T$ remains fairly linear within the entire temperature range, only one donor energy level is present: $E_d = 1.54$ eV.

Figure 6 shows a similar dependence of conductivity $\sigma(1/T)$ of sample #443 measured in the 4-point geometry. Conductivity activation energy E_σ at $T > 650$ K assumes a value of 1.64 ± 0.02 eV, which is virtually equal to the value of 1.63 ± 0.02 eV for sample #185. Energy $E_\sigma = 1.5$ eV for the #ND-2 sample is noticeably lower than the indicated

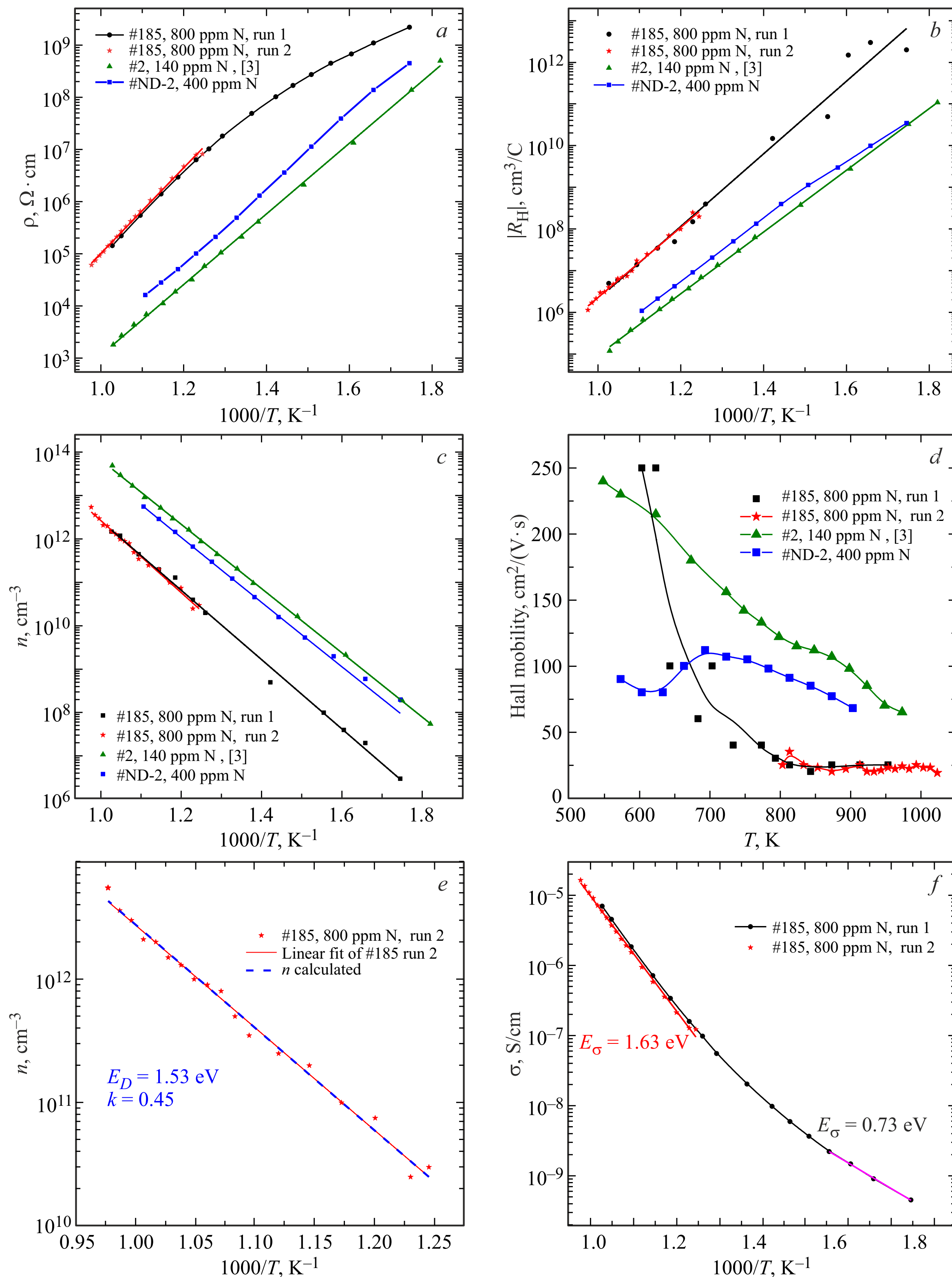

Figure 5. *a* — Resistivity ρ; *b* — Hall coefficient modulus $|R_H|$; *c* — concentration n of free electrons as a function of inverse temperature; and *d* — Hall electron mobility μ_H as a function of temperature. *e* — Dependence of concentration n of free electrons in sample #185 on inverse temperature within the 800−1020 K range. Symbols represent experimental points, the solid red line is the linear least-squares approximation, and the blue dotted line was plotted by solving electroneutrality equation (1), (2) with fitting of parameters E_d and k. *f* — Dependence of conductivity σ of sample #185 on inverse temperature in semi-logarithmic coordinates for determination of conductivity activation energy E_σ. The results of two independent measurement cycles are presented for sample #185. The data for sample #2 from [3] are provided for comparison.

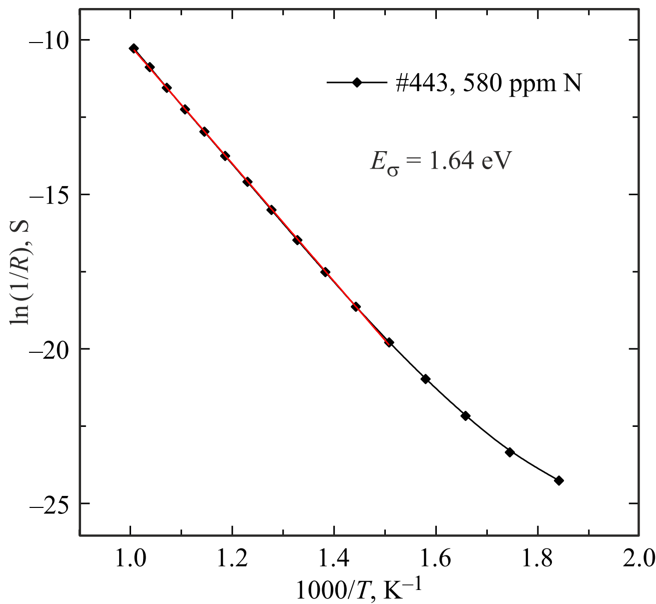

Figure 6. Dependence of conductivity σ of sample #443 on inverse temperature in Arrhenius coordinates.

values, but higher than the one determined for HPHT diamonds with a lower donor concentration in [3]. Donor ionization energy $E_d = 1.32$ eV in sample #ND-2 is virtually the same as the one in sample #5 from [3], which also had a high concentration of C-centers and high k. However, $E_d = 1.53$ eV in sample #185 is 0.1−0.2 eV higher than the values obtained for other HPHT diamonds.

It should be noted that sample #185 features a high compensation ratio: $k = (45 \pm 5)\%$. Neutral single nitrogen atoms in the substitutional position (C-centers) are considered to be the primary donors. Theoretical [36,37] and experimental [38] studies of the donor and acceptor properties of negatively and positively charged nitrogen atoms in the substitutional position in diamond have also been published.

The most well-characterized acceptor in diamond is boron, but its background concentration in all the studied samples does not exceed 10^{16} cm^{-3}, which is several orders of magnitude lower than the concentration of donors. Therefore, we do not consider boron to be the main acceptor impurity in our samples. As was noted in the Introduction, the acceptor properties of iron atoms, complexes of iron and nitrogen atoms in the substitutional position (Fe_s-N_s), and complexes of iron atoms with vacancies have recently been predicted theoretically in [24]. Impurity atoms of nickel and cobalt and complexes based on them may feature similar properties [39,40].

The low mobility of free electrons in sample #185 (~ 25 cm^2/(V$^{-1}\cdot$ s^{-1}) at $T > 800$ K; see Figure 5, d) is indicative of significant scattering by ionized impurities; the same was observed, e.g., in a single-crystal diamond sample doped with phosphorus at a concentration of $7.2 \cdot 10^{18}$ cm^{-3} with a compensation ratio of 93% in [33]. The mobility of free electrons in this diamond decreased to ~ 20 cm^2/(V$^{-1}\cdot$ s^{-1}). The electron mobility in sample #ND-2 reaches its maximum $\mu_{\mathrm{H}} = 125$ cm^2/(V$^{-1}\cdot$ s^{-1}) at $T = 700$ K and decreases smoothly to 70 cm^2/(V$^{-1}\cdot$ s^{-1}) at $T = 900$ K.

At a low concentration of free carriers, the concentration of ionized impurity centers is $N_{ii} \approx 2N_d$ in partially compensated hole semiconductors [33] and $N_{ii} \approx 2N_a$ [22] in electron semiconductors. Compensation ratios $k = 25$ and 45% determined experimentally for samples #ND-2 and #185 imply that $N_{ii} \approx 3.5 \cdot 10^{19}$ cm^{-3} for #ND-2 and $N_{ii} \approx 1.2 \cdot 10^{20}$ cm^{-3} for #185. We assume that this contribution to scattering in our samples may be greater than the one in the sample examined in [33], where $N_{ii} \approx 1.3 \cdot 10^{19}$ cm^{-3}. Scattering by ionized impurity centers is the dominant one in this sample in [33]. However, more accurate calculations with account for the difference in Debye screening lengths of the ion potential are needed in the case of diamond doped with nitrogen instead of phosphorus.

4. Conclusion

Three diamond single crystals with a concentration of substitutional nitrogen atoms (C-centers) within the $(0.7-1.35) \cdot 10^{20}$ cm^{-3} range were grown using the TG-HPHT method. Square thin plates were cut from two crystals to examine their electrical properties by the Hall effect method in the van der Pauw geometry. Ti−Pt metal contacts were deposited by magnetron sputtering onto all samples, and the linearity of their current–voltage characteristics within the 570−1000 K temperature range was verified. The dependences of resistivity and the Hall coefficient on temperature were investigated for two samples. The obtained data were used to calculate the temperature dependences of concentration of free electrons and their Hall mobility. The temperature dependence of conductivity was studied for the sample with a concentration of C-centers of $1.35 \cdot 10^{20}$ cm^{-3}. Linear sections of the dependences of $\ln(\sigma)$ on inverse temperature $1/T$ were observed at $T > 650$ K. Activation energies of conductivity $E_\sigma = (1.5-1.64)$ eV determined based on these sections are higher than those of TG-HPHT samples with a lower nitrogen concentration studied earlier in [3]. Moreover, the value of 1.64 eV is close to the known value of 1.7 eV for natural type Ib diamonds [1]. The dependence of $\ln(n)$ on $1/T$ for the sample with the highest nitrogen concentration remains fairly linear within the entire temperature range of 570−620 K and corresponds to $E_d \approx 1.53$ eV. This value is 0.1−0.2 eV higher than the donor activation energy in other diamond samples grown by the HPHT method in the present study and in [3]. In addition, this sample has the lowest concentration of free electrons among all the examined samples (within the entire temperature range) and the lowest electron mobility (at $T > 650$ K). Accordingly, it has the highest resistivity and the highest degree of

compensation of donor centers. The compensation ratio is as high as $(45 \pm 5)\%$ in the sample with a concentration of nitrogen C-centers of $1.35 \cdot 10^{20}\,\mathrm{cm}^{-3}$.

Thus, studies of the electrical properties of highly nitrogen-doped diamond single crystals grown by the HPHT method revealed a high degree of compensation of donor centers, which does not correspond to the background concentration of boron. This suggests the presence of other (presumably deep) acceptor centers. The increase in compensation ratio with increasing nitrogen concentration is also worth noting. This provides evidence of a correlation between the concentration of the main donor impurity (nitrogen in the substitutional position) and the concentration of compensating acceptor centers. Theoretical models of the energy levels of impurity iron atoms, complexes of iron and nitrogen atoms in the substitution position (Fe_s-N_s), and complexes of iron atoms with vacancies [24] demonstrate that such complexes may act as acceptors in diamond. Nickel and cobalt atoms in diamond and complexes based on them may have similar properties [39,40]. They may be the cause of significant compensation in TG-HPHT diamonds, which were examined in the present study and in [3]. A more thorough examination of the formation of metal impurity centers in HPHT-grown diamond single crystals and their energy spectrum should provide a better understanding of the electrical properties of semiconductor diamonds and help find a way to reduce the compensation ratio in highly nitrogen-doped diamonds and improve their semiconductor properties.

Acknowledgments

The authors wish to thank A. Galkin for measuring the IR spectra of samples. Equipment provided by the TISNUM collective use center (www.tisnum.ru/suec/suec.html) was used in the study.

Funding

Electrical measurements were performed with support from the Russian Science Foundation (research project No. 24-22-00385). The growth and spectroscopic characterization of certain crystals used in the study were carried out as part of the state assignment of the Sobolev Institute of Geology and Mineralogy of the Siberian Branch of the Russian Academy of Sciences (project No. 122041400159-3).

Conflict of interest

The authors declare that they have no conflict of interest.

References

[1] R.G. Farrer. Solid State Commun., **7**, 685 (1969).
[2] F.J. Heremans, G.D. Fuchs, C.F. Wang, R. Hanson, D.D. Awschalom. Appl. Phys. Lett., **94**, 15 2102 (2009).
[3] S.G. Buga, G.M. Kvashnin, M.S. Kuznetsov, N.V. Kornilov, N.V. Luparev, D.D. Prikhodko, S.A. Terentiev, V.D. Blank. Appl. Phys. Lett., **124**, 102107 (2024).
[4] H.B. Dyer, F.A. Raal, L. Du Preez, J.H.N. Loubser. Phil. Mag., **11**, 763 (1965).
[5] M. Kubovic, H. El-Hajj, J.E. Butler, E. Kohn. Diamond. Relat. Mater., **16** 1033 (2007).
[6] T. Matsumoto, T. Mukose, T. Makino. Diamond. Relat. Mater., **75**, 152 (2017).
[7] T. Matsumoto, T. Yamakawa, H. Kato, T. Makino, M. Ogura, X. Zhang, T. Inokuma, S. Yamasaki, N. Tokuda. Appl. Phys. Lett., **119**, 242105 (2021).
[8] M.A. Lobaev, D.B. Radishev, S.A. Bogdanov, A.L. Vikharev, A.M. Gorbachev, V.A. Isaev, S.A. Kraev, A.I. Okhapkin, E.A. Arhipova, M.N. Drozdov, V.I. Shashkin. Phys. Status Solidi RRL, **17**, 2000347 (2020).
[9] S.G. Buga, N.V. Kornilov, M.S. Kuznetsov, N.V. Luparev, D.D. Prikhodko, S.A. Tarelkin, T.E. Drozdova, V.D. Blank. Tech. Phys. Lett., **50** (3), 37 (2024).
[10] S. Salvatori, S. Pettinato, M. Girolami, D.M. Trucchi, M.C. Rossi. IEEE Trans. Electron Dev., **70** (5), 2330 (2023).
[11] I. Stenger, M.-A. Pinault-Thaury, T. Kociniewski, A. Lusson, E. Chikoidze, F. Jomard, Y. Dumont, J. Chevallier, J. Barjon. J. Appl. Phys., **114**, 073711 (2013).
[12] E.A. Ekimov, V.A. Sidorov, E.D. Bauer, N.N. Mel'nik, N.J. Curro, J.D. Thompson, S.M. Stishov. Nature, **428**, 542 (2004).
[13] Y. Takano. J. Phys.: Condens. Matter., **21**, 253201 (2009).
[14] Y. Ma, J.S. Tse, T. Cui, D.D. Klug, L. Zhang, Y. Xie, Y. Niu, G. Zou. Phys. Rev. B, **72**, 014306 (2005).
[15] E. Bustarret. Physica C: Superconductivity and its Applications (Elsevier, 2015) v. 514.
[16] F.J.R. Costa, J.S. de Almeida. J. Appl. Phys., **129**, 043903 (2021).
[17] J. Barzola-Quiquia, M. Stiller, P.D. Esquinazi, A. Molle, R. Wunderlich, S. Pezzagna, J. Meijer, W. Kossack, S. Buga. Sci. Rep., **9**, 8743 (2019).
[18] A. Setzer, P.D. Esquinazi, O. Daikos, T. Scherzer, A. Pöppl, R. Staacke, T. Lühmann, S. Pezzagna, W. Knolle, S. Buga, B. Abel, J. Meijer. Phys. Status Solidi B, **258**, 2100395 (2021).
[19] S.G. Buga, V.A. Kulbachinskiy, G.M. Kvashnin, M.S. Kuznetsov, S.A. Nosukhin, E.A. Konstantinov, V.V. Belov, D.D. Prikhodko. Diamond. Relat. Mater., **142**, 110759 (2024).
[20] Y.N. Palyanov, I.N. Kupriyanov, A. F. Khokhryakov, V.G. Ralchenko. Chap. 17, *Crystal growth of diamond, in Handbook of Crystal Growth*, ed. by P. Rudolph (Elsevier Science Ltd, 2015). ISBN 978-0-444-63303-3
[21] B. Gelmont, M.S. Shur. J. Appl. Phys., **78**, 2846 (1995).
[22] *Power Electronics Device Applications of Diamond Semiconductors. Woodhead Publishing Series in Electronic and Optical Materials*, ed. by S. Koizumi et al. (Woodhead Publishing, 2018) p. 178.
[23] N. Donato, N. Rouger, J. Pernot, G. Long. J. Phys. D: Appl. Phys., **53**, 093001 (2020).
[24] M.D. Alshahrani, J.P. Goss, P.R. Briddon, M.J. Rayson, C.V. Peaker. Diamond. Relat. Mater., **148**, 111332 (2024).
[25] Y. Borzdov, Y. Pal'yanov, I. Kupriyanov, V. Gusev, A. Khokhryakov, A. Sokol, A. Efremov. Diamond. Relat. Mater., **11**, 1863 (2002).
[26] Y.N. Palyanov, Y.M. Borzdov, A.F. Khokhryakov, I.N. Kupriyanov, A.G. Sokol. Cryst. Growth Des., **10**, 3169 (2010).

[27] S.G. Buga, G.M. Kvashnin, M.S. Kuznetsov, N.V. Kornilov, N.V. Luparev, M. Yao. Semiconductors, **57** (5), 360 (2023).
[28] M.N.R. Ashfold, J.P. Goss, B.L. Green, P.W. May, M.E. Newton, C.V. Peaker. Chem. Rev., **120**, 5745 (2020).
[29] U.F.S. D'Haenens-Johansson. J.E. Butler, A.N. Katrusha. Rev. Mineral. Geochem., **88**, 689 (2022).
[30] A.M. Zaitsev. *Optical properties of diamond: a data handbook* (Springer, Berlin-N.Y., 2001).
[31] M. Katagiri, J. Isoya, S. Koizumi, H. Kanda. Appl. Phys. Lett., **85**, 6365 (2004).http://dx.doi.org/10.1063/1.1840119
[32] H. Kato, M. Ogura, T. Makino, D. Takeuchi, S. Yamasaki. Appl. Phys. Lett., **109**, 2102 (2016).
[33] I. Stenger, M.-A. Pinault-Thaury, N. Temahuki, R. Gillet, S. Temgoua, H. Bensalah, E. Chikoidze, Y. Dumont, J. Barjon. J. Appl. Phys., **129**, 105701 (2021).
[34] J.S. Blakemore, in Semiconductor Statistics, ed. by H.K. Henisch (Pergamon Press, 1962).
[35] N. Naka, K. Fukai, Y. Handa, I. Akimoto. Phys. Rev. B, **88**, 035205 (2013).
[36] R. Jones, P. Goss, P. R. Briddon. Phys. Rev. B, **80**, 033205 (2009).
[37] A. Platonenko, W.C. Mackrodt, R. Dovesi. Materials, **16**, 1979 (2023).
[38] R. Ulbricht, S.T. van der Post, J.P. Goss, P.R. Briddon, R. Jones, R.U.A. Khan, M. Bonn. Phys. Rev. B, **84**, 165202 (2011).
[39] A.T. Collins, Diamond. Relat. Mater., **9**, 417 (2000).
[40] A. Elisseyev, H. Kanda. New Diamond. Front. Carbon Technol., **17** (3), 127 (2007).

Translated by D.Safin